Inspection of reinforced and prestressed concrete strutures through an ultrasonic technique performed by ultrasound tomograph - Mira

By Maria Roque; November, 2014

Abstract

When performing rehabilitation of a structure it is relevant to have inspection techniques to analyze the condition of the structure. Where possible, it is preferable to use non-destructive inspection techniques because, unlike the destructive inspection techniques, the former allow performing an analysis without damaging the structure. Technological developments have enabled high advances in non-destructive techniques for structures inspection. The ultrasonic tomograph - Mira is an innovative and non-destructive equipment used to obtain images of the interior of the concrete which is based on the detection of contrast and density through ultrasound. This equipment contains 40 piezo-electric transducers of dry spot contact using shear waves of low frequency. When operating, the transducers act as transmitters and receivers in a sequential mode. Using the synthetic aperture focusing technique, a 3D model and 2D cuts of the section are obtained, allowing the observation of geometry of the object under test as well as the location of existing reinforcement and, more importantly, the location of internal defects such as voids, cracks or forming "honeycombing". This dissertation aims to evaluate a non-destructive technique for the inspection of reinforced and prestressed concrete structures. Specifically it aims to check the effectiveness level of ultrasonic tomography MIRA in determining thickness of the object under study, in identifying the location of existing reinforcement, descontinuities and voids within the concrete. Four prototype beams, two concrete and two reinforced and prestressed concrete were analyzed, with the ultrasonic tomograph – Mira. The four beams had simulated defects, including i) cracks; ii) voids in concrete; iii) honeycombing and iv) voids in prestressing ducts. In the concrete beams, results allowed to visualize the location of all existing singularities and, in cracks, it also allowed to dimension them. In the reinforced and prestressed concrete beams, rebars, prestressing cables, cracks and honeycombing were visualised. It is concluded that this technique would be ideal for an initial analysis for inspecting a structure since it identifies the existence of anomalies and locates them.

1. Introduction

At present one of the priorities in the construction sector is the durability of constructions and materials. Under this framework, rehabilitation of structures is of great importance. Concrete has been used intensively in the last century and today there is an awareness that the concrete gets old over time, suffering from deterioration which decreases its strength. Considering additionally the possible design errors, construction errors and/or changes in structure use, the need for structural rehabilitation in reinforced and prestressed concrete is increasingly present. The rehabilitation of a structure presupposes the analysis of its geometric features, materials and condition. The characterization of the structure requires the use of inspection techniques to analyze its condition. These can be made by destructive methods – involving the collection of samples for testing, causing damage to the structure; or by non-destructive methods – these are preferable because they allow performing an analysis without damaging the structure. These two kinds of methods can also be used in combination for a better collection of the information. One of non-destructive techniques used consists in evaluating the velocity of ultrasounds propagation along a given alignment. Changes occurring in the velocity of propagation enable to evaluate discontinuities in the concrete. The ultrasonic tomography Mira is a non-destructive technique that uses ultrasound to obtain images of the interior of the element being analyzed to assess the state of the element and its geometry. The aim of this work is the generation, analysis and interpretation of these images.

2. State-of-the-art review

The tests using ultrasound are based on the theory of wave propagation. According to this theory when a solid medium is disturbed by a vibrating action there are two main types of waves: volume and surface waves. Volume waves are divided into longitudinal (or compression) waves and transverse waves (or shear). The ultrasonic tomograph - Mira uses fundamentally low frequency shear waves. Ultrasound is generated through the transducers i.e. piezoelectric elements. The assay uses an ultrasonic device capable of transforming an electrical pulse of mechanical waves through the transducers. As seen in Figure 2.1, the waves are transmitted (transmitting transducer) to the material where they are propagated and they are received by a receiving transducer. As the waves propagate along the material, the mechanical vibration of these waves will attenuate due to the combined effect of absorption and scattering. When the wave falls on the surface of separation of two different media, it is partly reflected and partly transmitted to the second medium (figure 2.2) [Luz et al.., 2013]. In the case where the wave falls on obliquely, apart from splitting into reflected and transmitted waves, it also suffers an offshoot, which means that the wave forms a reflected longitudinal wave and a transmitted longitudinal wave and a further reflected transverse wave and a transmitted transverse wave (figure 2.3). The angles of reflection and refraction are given by Snell's Law.

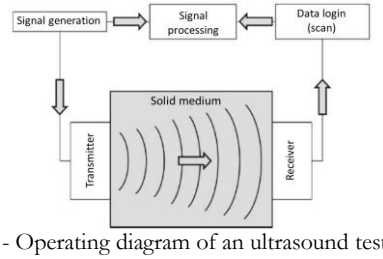

Figure 2.1- Operating diagram of an ultrasound test [Rio e Figueiras, 2012]

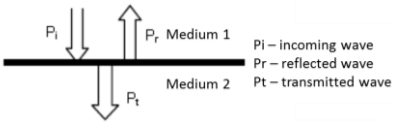

Figure 2.2- Transmission and reflection [Luz et al., 2013]

Lei de Snell:

$$\frac{\text{sen } \theta 1}{Pl1} = \frac{\text{sen } \theta 2}{Pl2} = \frac{\text{sen } \theta 3}{Pt1} = \frac{\text{sen } \theta 4}{Pt2}$$

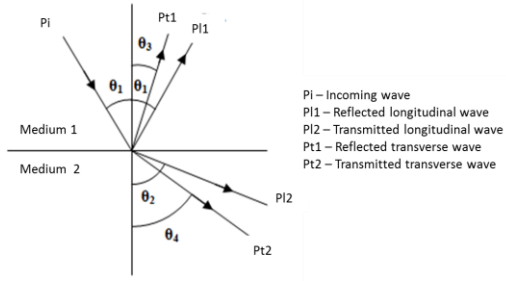

Figure 2.3- Oblique incidence at an interface between two different media [adapted from Luz et al., 2013]

The study of wave propagation through an interface between two different media is important to study the discontinuities in the concrete, since when a wave propagates in a homogeneous medium, all particles vibrate in an identical manner but when the wave propagates in a not perfectly homogeneous medium reflections and refractions occur that alter the path of the wave [Luz et al.., 2013].

In the procedures and interpretation of results obtained in a test performed with an ultrasound it is important to consider some factors that may influence the results and lead to incorrect conclusions [Naik et al., 2004]: i) aggregate size, grading, type and content; ii) cement type; iii) water/cement ratio; iv) admixtures; v) age of concrete; vi) transducer contact; vii) temperature of concrete; viii) moisture and curing condition of concrete; ix) path length; x) size and shape of a specimen; xi) level of stress; xii) presence of reinforcing steel.

In a test, obtained images of the inside of concrete can be of three types (depending on equipment): A, B and C scan, shown in Figure 2.4. Figure 2.5 shows positions of different image modes A, B or C scan. Information obtained by A-scan is one-dimensional and refers to the path followed by the ultrasound. The measured propagation time indicates depth at which the defect is located and an analysis of the received signal amplitude estimates the size of the defect.

In the obtained image, the horizontal axis shows delay time and vertical axis shows amplitude [Schickert et al., 2003]. In the case of B-scan, the transducer moves along one axis and obtains a cut parallel to propagation direction (several A-scans in same axis). A-scan's amplitudes are converted to colors or gray scale and placed side by side. The image obtained is two-dimensional and the horizontal axis shows the

distance along inspection direction and the vertical axis shows the distance along the ultrasound path [Schickert et al., 2003]. In C-scan, the performed scanning is in a defined plane, perpendicular to the

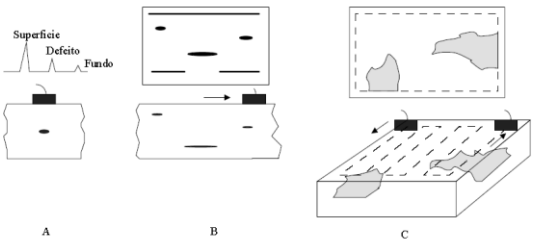

Figure 2.4- Obtained information by the methods A, B and C scan [Santos, 2004]

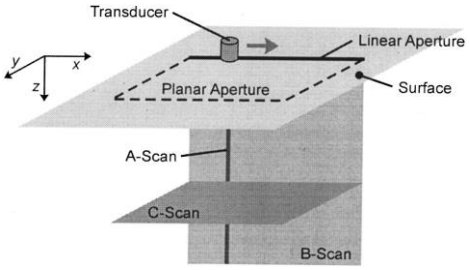

Figure 2.5- Positions of the images modes [Schickert et al., 2003]

propagation direction. Signals are collected for each point in the plane (several B-scans in same plane) which allows the image construction [Santos, 2004]. Existing systems use a computer to monitor either excitation or movement of the transducer, signal acquisition and desired image presentation. The main techniques of ultrasonic imaging used today are based on the operating principles of the methods B and C-scan. The imaging technique used by the ultrasonic tomograph - Mira is a synthetic aperture focusing technique that, by processing received signals, constructs a 3D model and 2D cuts of the section in the three main directions.

The Germann Instruments company conducted tests on a concrete slab with two inserted ducts, one injected and another empty. Results obtained by the tomograph Mira are presented in figure 2.6. As figure 2.6 shows, both ducts are perfectly identifiable and locatable. It is worth noting that the injected duct is in fact not full, at one side, as the red reflection indicate, that there is air in the duct. Reinforcement is also identifiable. This slab was tested with a second appliance and it was found that the obtained results were similar to the results obtained with the Mira aparatus. Tests were also performed to assess the presence of voids in a steel box girder bridge that was overlaid with of fiber-reinforced concrete. Figure 2.7 shows results obtained. Red regions represent possible presence of voids. Subsequent drilling confirmed the results of the Mira tomograph.

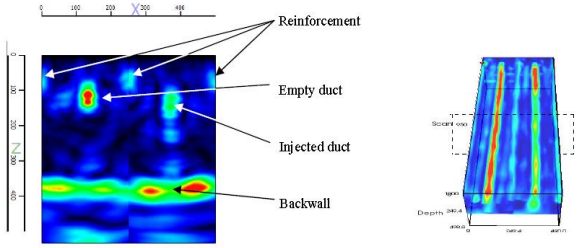

Figure 2.6- B-scan - reflection at 1,2m from the slab beginning. 3D illustration showing the location of B-scan[Germann Instruments, 2011]

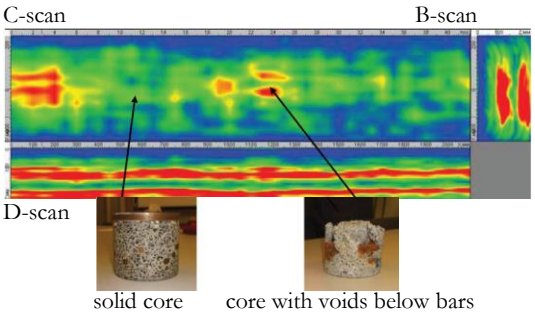

Figure 2.7 - Results obtained by the tomograph Mira and concrete samples in two distinct zones [Catalog NTD, 2010]

In tests conducted using the Mira tomograph to a foundation slab, it was found that the thickness of the slab was not the same defined in design, and it was reinforced for safety reasons.

3. Experimental Study

Tests using the ultrasonic tomograph - Mira were performed to obtain images that enabled to interpret the interior of the structural element under study.

Two concrete beams (figure 3.1) and two prestressed concrete beams (figure 3.2) were designed and built. The last two simulated beams in service in a real situation, with the particularity that their ducts were already in advanced corrosion process. Pathologies of common situations in this type of structures were recreated and it was about them that tests focused [Almeida et al. 2012].

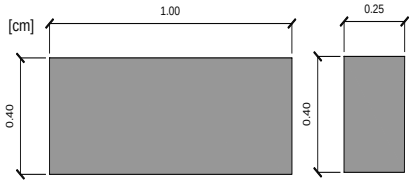

Figure 3.1 - Geometry of concrete beam (prototypes A and B)

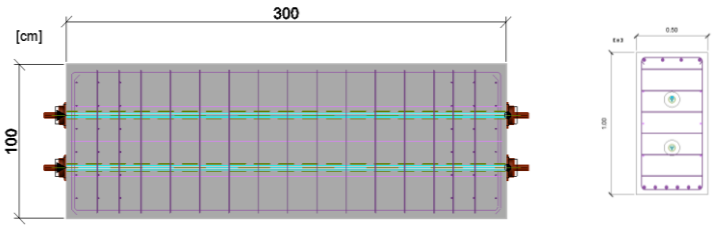

Figure 3.2– Geometry of prestressed concrete beams (prototypes 1 and 2)

The execution of the four analyzed prototypes was guaranteed by the building company Teixeira Duarte.

Figure 3.3 illustrates the concrete beams, prototypes A and B. Three rebars with diameters of 6, 12 and 25 mm and four plastic tubes with diameters of 10, 20, 30 and 40 mm in order to simulate cylindrical voids, were placed in prototype A. Four cracks and one "honeycomb" were simulated in prototype B. All simulated anomalies were located in well-defined positions in order to facilitate the interpretation of test results.

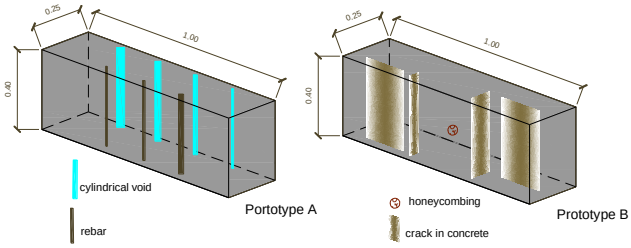

Figure 3.3 - Singularities of concrete beams

In reinforced and prestressed concrete beams (prototypes 1 and 2) two cables were inserted containing 3 strands, stretched to 500 kN. The prestressing was applied by post-tensioning. Active anchors were used in one of the ends of the beam and passive anchors at the opposite end. Defects in execution and high chloride concentration in the grout of ducts were simulated. In these prototypes there were also simulated some pathologies such voids in grouting of prestressed tendons, voids, "honeycombing" and cracks in concrete, all of known dimensions and locations. These defects simulated the main and most common construction and durability anomalies found in this type prestressed concrete structures.

Figure 3.4 A shows that the execution of both beams steel bars with evident corrosion of rebars and ducts. In the prestressed ducts voids were left (figure 3.4 B) properly identified and executed by placing plastic tubes that support across the ducts at desired locations. Within each tube, a steel bar that entered into the duct was inserted. The bar was removed after setting the grout. To create voids in concrete, tiles typically used in swimming pools were used. Due to its flexibility, tiles were molded to create air pockets and it was surrounded by a watery cement paste to maintain the desired shape. As seen in Figure 3.4 C a very thin plastic sheet was placed in order to cover part of the section to simulate the existence of a crack. Honeycombing were performed using stockings (thin permeable) filled with crushed stone and attached to the reinforcement at the marked points in the project (Figure 3.4 D) [Almeida et al., 2013].

A B C D

Figure 3.4 – A - Corrosion of reinforcement and ducts. B – Voids in prestressed ducts marked in red, where one cross tube will be placed. C - Blade plastic marked in red that simulated a crack. D - Simulation of a honeycomb [Almeida et al., 2013]

Figure 3.5 shows the relative location of the singularities in the beams under study, through their representation on the outer face of the beam in three dimensions.

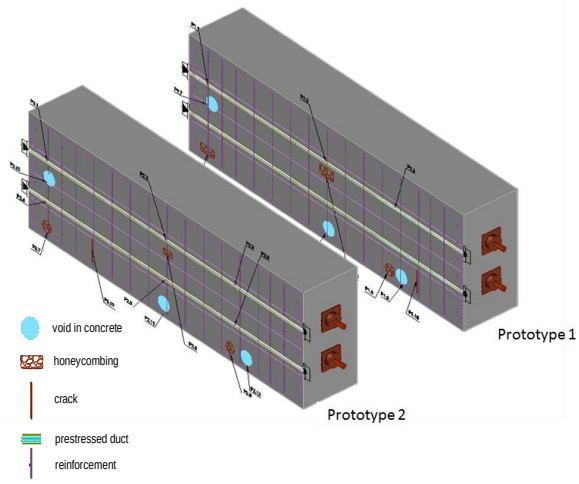

Figure 3.5 - Spatial representation of singularities in prototypes 1 and 2

Prototype 1 has three voids in the concrete, with similar dimensions; three honeycombing, one of which has a spherical shape and two other parallelepiped; three voids in prestress duct, all located on the upper duct and, finally, a crack at the bottom of the beam. Prototype 2 has three voids in concrete of similar dimensions; three honeycombing, one of which has a parallelepiped shape and two spherical; six voids in prestress duct, three located in the upper duct and three in the lower duct, finally; a crack at the bottom of the beam. All simulated anomalies were located in well-defined positions in order to facilitate the interpretation of test results.

The device used to obtain images of the interior of the concrete was the ultrasonic tomograph Mira, developed by Germann Instruments. It works based on detection of contrast and density system through ultrasound. The main parts of the equipment are the antenna array and the laptop with a monitoring and data program installed (Figure 3.6). The antenna array has 40 shear wave low frequency transducers, disposed in a 10 x 4 (10 rows, 4 columns) matrix. The transducers are spring-loaded to conform to an irregular surface, dry-point contact piezoelectric sensors with a center frequency of 50 kHz. Each transducer is built with a wear-resistant ceramic tip, which allows testing even on very rough surfaces. In operation, the transducers act as transmitters and receivers in a sequential mode. In summary, the control unit within the antenna excites one row of transducers and the other rows of transducers act as receivers [Catalog NDT, 2010]. Figure 3.7 shows the 45 rays paths involved in each of the four columns of transducers. It takes less than 3 seconds to complete data acquisition, data processing, and data transfer for a test at one single antenna location. The program installed on the laptop allows, through the wireless connection to the antenna, receiving signals obtained by the antenna, process and archive them as data [Catalog NDT, 2010].

Figure 3.6 - Antenna and laptop with control and analysis program. [Catalog NDT, 2010]

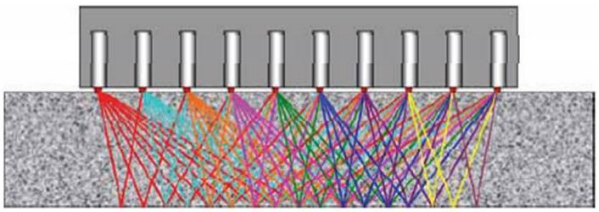

Figure 3.7 - 45 rays paths that are involved in each of the four columns of transducers

Using the synthetic aperture focusing technique, a front view, a cross section, a longitudinal section and a 3-D model are constructed, also allowing the location of the opposite side of the test object (Back wall reflection), the location of existing reinforcement and, more importantly, the location of internal defects such as voids, cracks or honeycombing.

Images presentation on the computer is performed according to the axis antenna system as shown in Figure 3.8 and images generated by the software are presented in Figure 3.9.

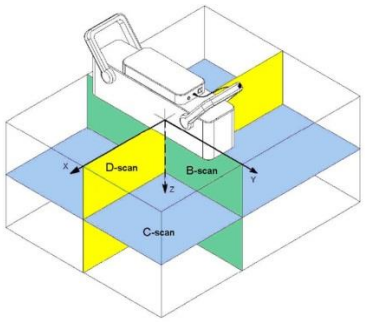

Figure 3.8 - Planes and axes antenna system [Manual Mira, 2010]

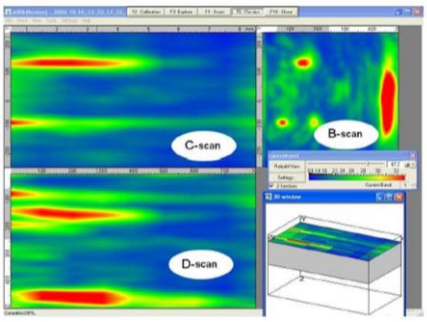

Figure 3.9 - Images generated by the sofware [Manual Mira, 2010]

Tests were based on making scans in both directions in the test object different faces. The aim was defining ways of interpreting obtained images of the existing anomalies. The general procedure consisted of the following steps: **i**) visual inspection to confirm element surface planarity and roughness; **ii)** test element surface preparation to be inspected; surfaces that come into contact with the antenna have to be free of any dust or sand and materials with different physical characteristics from concrete (eg paints and sealants) removed; **iii)** mark the study element with a area scan map (figure 3.10); **iv)** confirm if program is installed in computer, if all units are properly connected and if tomograph and computer batteries are loaded; **v)** turn on tomograph and computer, wait 1-2 minutes for the wireless connection between the antenna and the computer is active; **vi)** performing calibration (Figure 3.11 A) (propagation velocity is automatically measured); **vii)** explorer mode (single scan) specify concrete thickness to analyze and step for performing scans; **viii)** testing in explore mode in 1 or 2 different positions to confirm configuration of the device (Figure 3.11 B); **ix)** scan mode (multiple scanning), performing the 1st scan. At each antenna location change, take care seeing if all transducers are snug against the face (Figures 3.11 C and 3.11 D); **x)** select review mode where there are recorded and processed data acquired during the scan performed. Record this data in another directory and another file name. Recording JPEG images obtained is also performed in this mode (Figure 3.9); **xi**) analyze obtained images; **xii)** if the images obtained are not very clear or are barely perceptible it is possible to change the frequency and the "gain" which changes the obtained images intensity. All other parameters should not be changed.

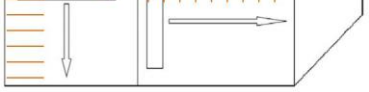

Figure 3.10 - area scan map

A B C D

Figure 3.11 - A - Calibration. B - Explorer mode test. C, D - Scan mode test.

The tomograph may be used between 0 and 45 ° C, which, in Portugal, allows its use in almost any time and any place. The equipment is not heavy and is easy to use, being able to perform multiple scans one after another.

In the present study all types of anomalies were covered, namely voids in concrete, voids in prestressed ducts, cracks and honeycombing. The intention was thus to evaluate which are the most easily identifiable anomalies using this non-destructive method and how each one is expressed in the obtained images.

4. Results and discussion

In this section the results of the experimental study are presented and discussed. The analysis consisted essentially in the interpretation of the images obtained through the ultrasound tomography technique.

The first tests were performed at concrete beams (prototypes A and B) for being simple beams, precisely designed to test the Mira tomograph ability. These beams were not reinforced and had a reduced number of anomalies, sufficiently far apart not to be easily confounded. Horizontal and vertical scans of the various faces of each beam were performed.

Tests in these beams were performed inside the Laboratório de Estruturas e Resistência de Materiais (LERM) in Engenharia Civil pavilion of Instituto Superior Técnico, thus maintaining significantly constant environmental conditions throughout all scans.

Flatness, roughness and size were taken into account in the analysis of the scans results, expecting resulting images to show higher or lower clarity depending on those same features.

The sofware allowed displaying the same image with higher or lower intensity (decibels adjusted) which facilitated its interpretation. Recording of the obtained images was performed in JPEG format, which enabled post processing.

The faces of the beams A and B were inspected to assess the surface's flatness and roughness. As observed in Figures 4.1 and 4.2, the faces are apparently flat. The sides 1, 3 and 4 are less rough when comparing with side 2, which has a higher roughness (free face during the concreting process).

Figure 4.1 - Prototype A various faces

Figure 4.2 – Prototype B various faces

Figure 4.3 - Peeling and delamination in the prototypes

Some few vertices and edges of both beams were peeled or delaminated at various locations (Figure 4.3).

Images obtained by the tomograph are presented according to antenna axes. In order to facilitate images understanding and interpretation, an illustration is presented representing each section according to antenna axes. In beam A, brown color represents rebars and blue color represents voids. In beam B, cracks are shown in brown and honeycombed in blue. The dashed pink line was placed on the image to indicate back wall. When analyzing the results of the tests performed on prototype A, it is possible to conclude that tests performed on opposite faces show similar results.

Images obtained in each scan by the tomograph are presented in figures 4.4 to 4.8, as well as an illustration with antenna tomograph location and illustrations representing the various cuts.

In any tests both B-scan and D-scan easily identify the back wall by the spot which appears at 250 mm. The spot is produced by surface ultrasonic reflection in the free face.

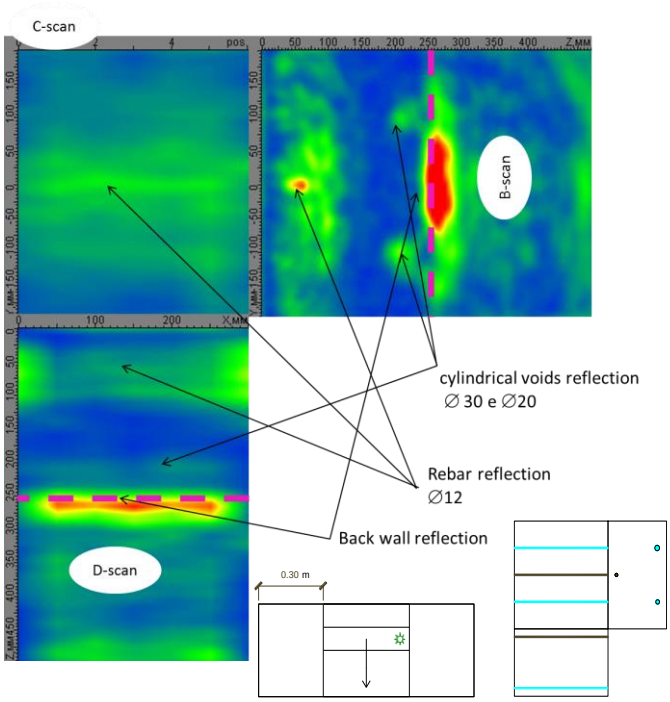

Figure 4.4 - Images from test VAF1H5Y30

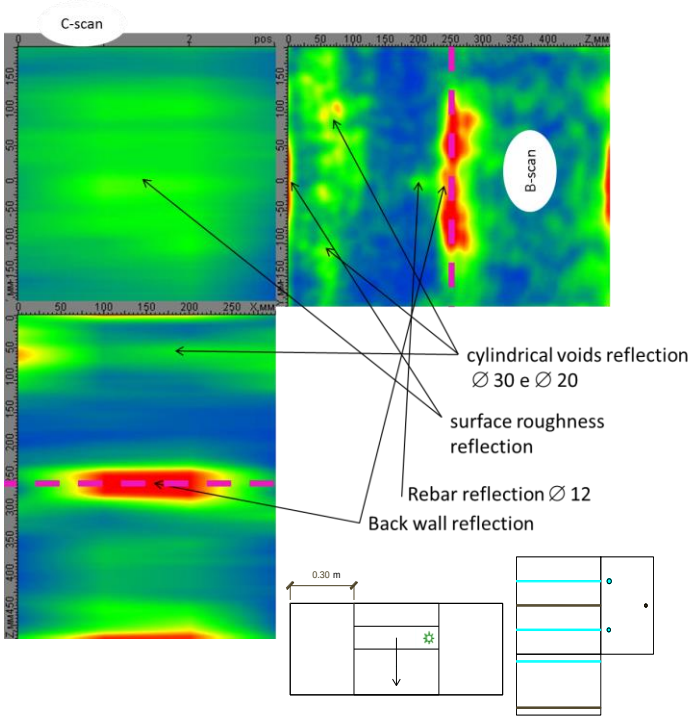

Figure 4.5 - Images from test VAF2H10Y30

In test VAF1H5Y30 (figure 4.4) performed on beam A, face 1 with a scan step of 5 cm, on B-scan, rebar and voids are perfectly clear. Image shows location of both rebar and voids but it is not possible to be accurate in their dimensions. In the D-scan is also possible to identify the development of voids and rebar.

Test VAF2H10Y30 (Figure 4.5) was carried out on beam A, face 2 with a scan step of 10 cm (opposite face of previous test, which has a higher roughness). On B-scan, rebar and voids are visible but are not as clear as in the previous test (VAF1H5Y30), which seems to be due to surface roughness in contact with the tomograph. This roughness translates into the loss of image sharpness of C-scan and visible reflections on B-scan, as seen in Figure 4.5. In the D-scan it is also possible to identify the development of voids quite clearly.

Due to the lack of sharpness in the initial test VAF2H10Y30 a 3D model is presented (option given by the software program) in cutting B-scan roughly at half the height of the beam prototype A (Figure 4.6). This was,

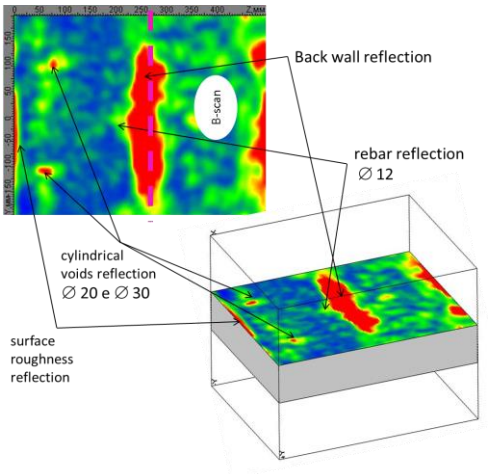

Figure 4.6- Images from test VAF2H10Y30 roughly half the height of the prototype A

in the present test, the sharpest image. The location of the rebar and the voids still were not as well defined as in the tests carried out on face 1.

In test VBF1H10Y60 (figure 4.7) performed on beam B, face 1 with a scan step of 10 cm, on B-scan crack (P1.1) is identified and located and it is possible to measure approximately its length (approximately 20 cm). On C-scan the crack appears in parallel plane to the image, being recognized by the roughly diffuse green spot.

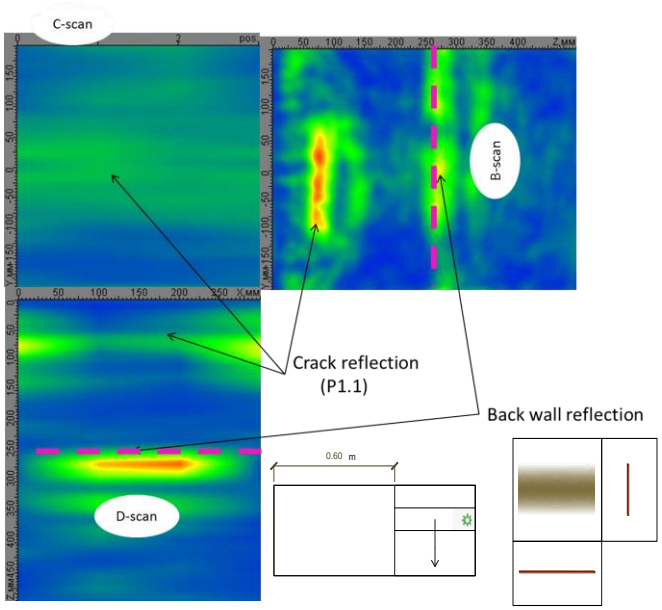

Figure 4.7 - Images from test VBF1H10Y60

When identified in a perpendicular plane to the crack itself (B-scan and D-scan), the expression of the crack shows a high thickness, which does not correspond to reality. On C-scan and on D-scan it is understood that the crack is nearly over the entire height of the beam.

Finally, in test VBF1V2X0 (figure 4.8), carried on beam B, face 1, it is possible to identify and locate virtually any existing cracks on C-scan and on D-scan. The identification of honeycombing is less obvious, although this singularity appears to have visible expression on D-scan, as indicated in the figure. This test was performed with smaller scan step, equal to 2 cm, to enable to identify the vertical cracks (P1.3 and P1.4), which appears to have resulted in better identification and definition of singularities.

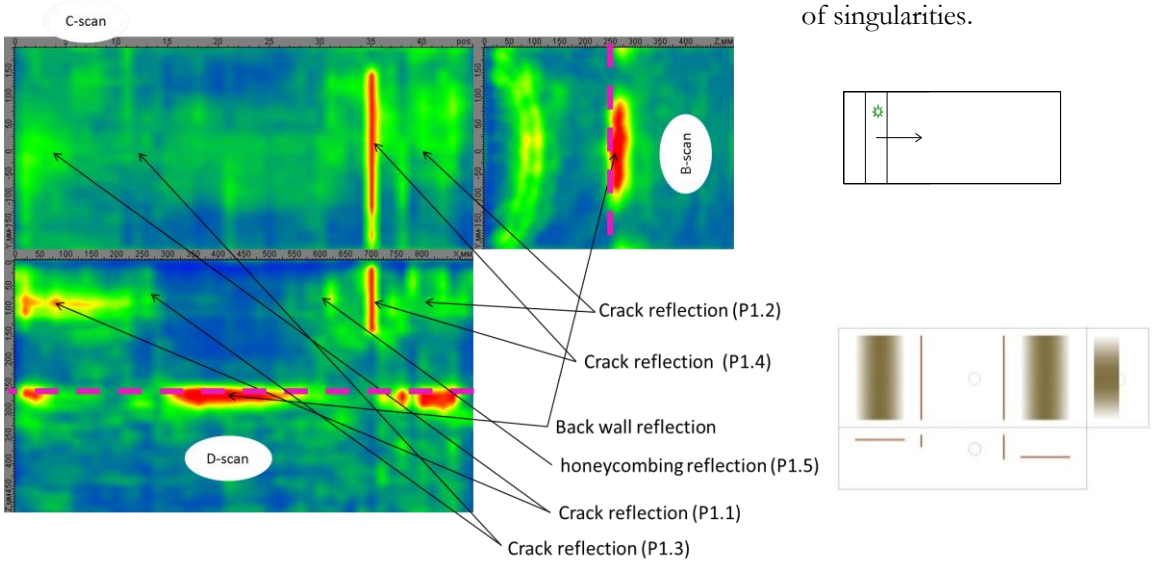

Figure 4.8 - Images from test VBF1V2X0

Tests for reinforced and prestressed concrete beams (prototype 1 and prototype 2) were performed in the Operational Polo of the building company Teixeira Duarte in Montijo, outdoors. Visual inspection of the faces, showed that they are not quite flat and there is significant roughness (figure 4.9), even in formwork faces.

Figure 4.9 - Prototypes 1 and 2 faces

On these beams, scans were made with antenna in vertical position due to: i) it is easier to scroll through a beam with the antenna in that position; ii) the lack of flatness of faces (Figure 4.9) hinders the transducers of being all snug against the face, when the antenna is horizontal.

The first images obtained for these beams were not clear and it was found that, after calibration, the value of "gain" was very high, therefore making it necessary to try lower these values, and several attempts were made. Images obtained in each scan by the tomograph are presented in figures 4.10 to 4.12 as well as an illustration with tomograph antenna location and illustrations representing the various cuts. Again a dashed pink line was used to identify the back wall, blue for voids, brown for cracks and honeycombing and green for prestressing cables.

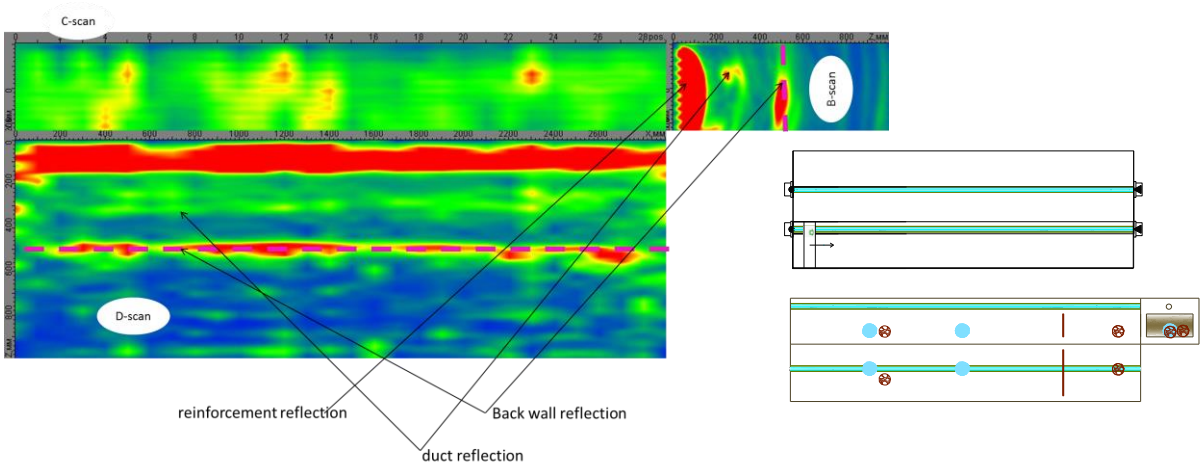

Figure 4.10 - Images from test V2F2V10X0

Test V2F2V10X0 was performed on beam 2, face 2 with a step of 10 cm. Figure 4.10 was obtained with very high "Gain" and in order to allow seeing more than a red spot, intensity was lowered (decibels adjusted). The back wall is identified by the red spot at 0.50 m. On D-scan it is possible to locate the prestressing cable. However, it is not possible to locate existing anomalies. On C-scan, existing reinforcement can be perceived, but anomalies in the predicted places are not identified. On B-scan the first red spot might be the reflection of the existing reinforcement near the face and a small red spot followed by smaller one might be the prestressed cable.

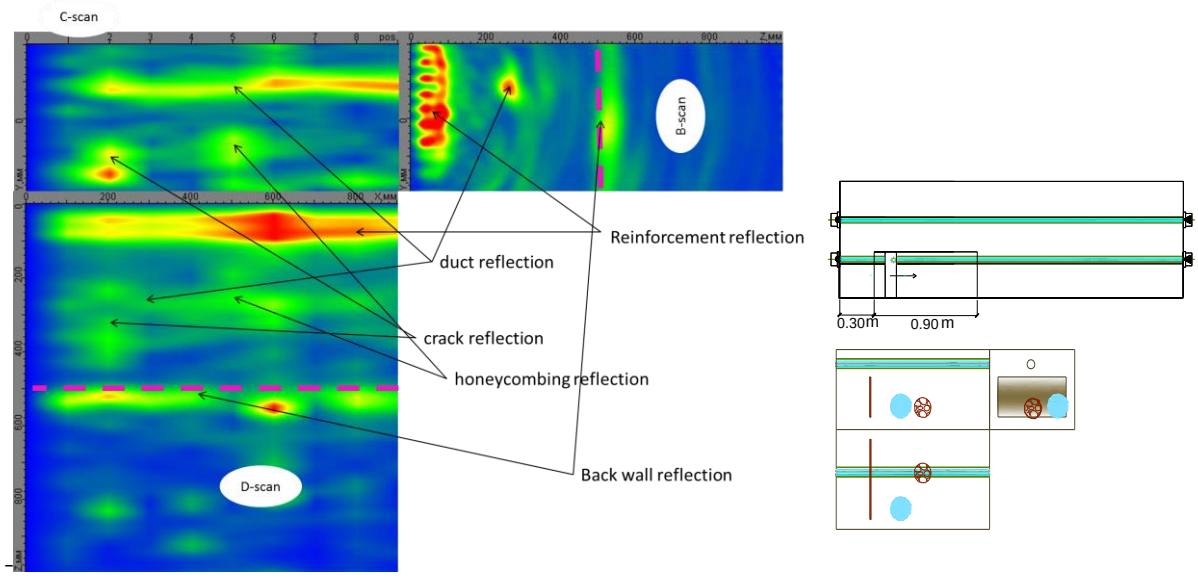

Figure 4.11 - Images from test V1F2V10X0

Test V1F2V10X0 was performed on beam 1, face 2 with a scan step of 10 cm in an area of 80 cm, in which different singularities are found (one crack, one void, one honeycombing and the prestressing cable). Figure 4.11 was obtained after changing "Gain" value. The back wall is again identified by the spot at 0.50 m. The C-scan of this figure is a plane about half of the girder thus the crack and the honeycomb

are only visible beyond the prestressing cable. On B-scan, reinforcement and prestressing cable can be identified. On D-scan besides the prestressing cable and reinforcement, the honeycombing reflection and the crack reflection are also visible.

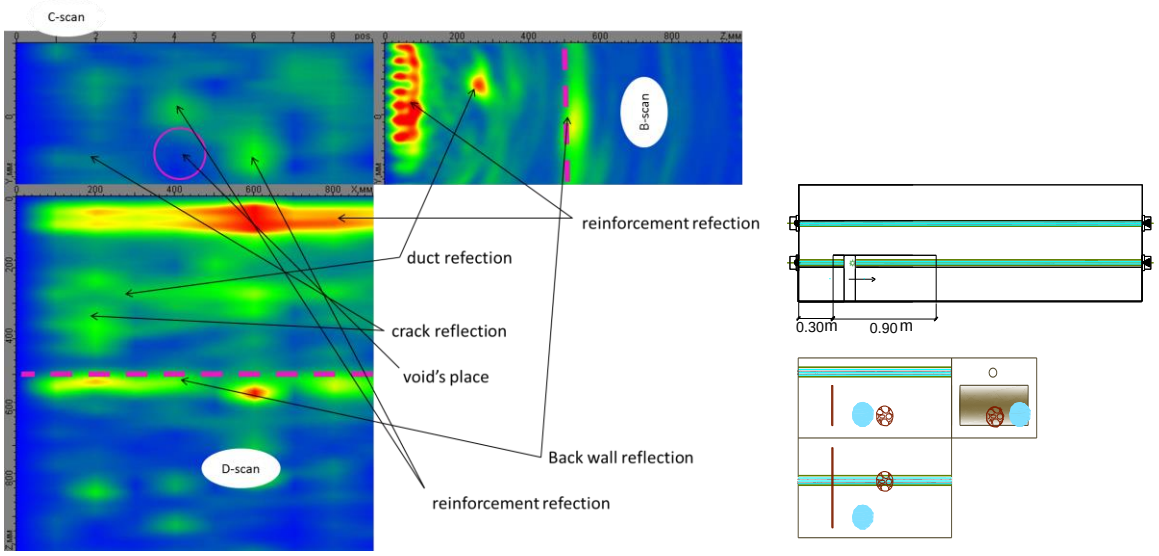

Figure 4.12 - Images from test V1F2V10X0

Figure 4.12 was obtained from the same test as shown in Figure 4.11 but the C-scan of this figure is a plane near the face where the void is located so the honeycombing is not visible but the crack is. The void can not be identified, but the reinforcement becomes more visible at the the void location. On B-scan the reinforcement and the prestressing cable are identified. On D-scan, besides from the reinforcement and the prestressing cable, the crack also visible. Back wall spot is identified at 0.50 m.

In this experimental campaign, the most significant differences between the tests are due to the condition of the surface where scanning is performed and differences on step used in scan. As a rule, the step used is 10 cm (the width dimension of the antenna), but it does not always provide accurate images. Normally, reducing the step allows obtaining better quality images.

The results obtained through the use of an ultrasonic tomograph in the prototypes A and B show the identification of the location of all singularities of the beams - rebars, voids, cracks and honeycombing. It was, however, not possible to clearly identify the type of anomaly through the images. There is, for example, a rebar which may look similar to the ultrasonic tomography image of a cylindrical void. Apparently, any change in material density that is under observation causes an increase in image intensity adjusted in decibels.

In prototypes 1 and 2, those beams which were more similar to reality beams, it was more difficult to obtain acceptable results. In these beams it was necessary to take into account the parameters derived from the calibration. It was not possible to identify voids in concrete or voids in prestressed ducts, although in Figure 4.11, where prestress cable reflection is shown in red, it is possible to assume the existence of air in the duct which it is not an introduced anomaly. It is again not possible to identify the type of anomaly through the image.

5. Conclusions

The ultrasound technique applied to prototype beams A and B proved to be a valid form of identification of current anomalies in concrete structure because, in spite of being unable to clearly identify the type of anomaly, it was possible to identify the location of all singularities existing and, in case of cracking, of its dimensions.

The same technique applied to prototype beams 1 and 2 (reinforced and prestressed concrete beams) was also valid in the identification of reinforcement and prestressing cable, honeycombing and cracks. However, it did not identify neither voids in concrete nor voids placed in prestressed ducts. It was also not possible to identify the presence or absence of corrosion in either reinforcing bars or prestressing cables.

In further studies, it would be important to smooth the prototypes faces and to perform new scans trying to improve resulting images. It would also be important to remove samples from the prototypes in order to verify concrete homogeneity, especially in prototypes 1 and 2 where a red zone appears (possible voids) near reinforcing and where it was more difficult to locate existing anomalies. One should also check the existing voids in the prestressing ducts.

The ultrasound tomograph - Mira has as main advantages: being non-destructive; lightweight; easy to transport and easy to apply. Obtaining and processing images in a short time (it takes less than 3 seconds to complete data acquisition, data processing, and data transfer for a test at one antenna location.); obtain images in 3 planes and in 3D which allows better visualization of the interior of the concrete.

This technique would be ideally used in an initial inspectory analysis of the structure, since it identifies the existence of anomalies and locates them, thus indicating where the use of other techniques for identifying the kind of anomaly is required.

6. Acknowledgements

The author acknowledges support from the Teixeira Duarte S.A company.

References

- Almeida, A., Duarte, F., Caldas, J., Moura, R., Xavier, B., 2012 – Tomografia e reabilitação de estruturas de betão armado e pré-esforçado. Reabeat, projecto dos protótipos, memória descritiva e justificativa. Teixeira Duarte, Engenharia e Construções, S.A.
- Almeida, A., Duarte, F., Caldas, J., Moura, R., Xavier, B., 2013 – Tomografia e reabilitação de estruturas de betão armado e pré-esforçado. Reabeat, relatório de execução dos protótipos. Teixeira Duarte, Engenharia e Construções, S.A.
- Catalog NDT, 2010 - NDT Systems. Germann Instruments.
- Germann Instruments, 2011 - Injection of cable ducts evaluated by MIRA ultrasound and DOCter impact-echo. Germann Instruments.
- Luz, A., Santos T., Barros P., Vilaça P., Quintino L., - Concepção desenvolvimento e produção de sondas de ultra-sons. Instituto Superior Técnico de Lisboa e Instituto de Soldadura e Qualidade.
- Manual MIRA, 2010 - MIRA – Tomographer, Germann Instruments.
- Naik, T.R., Malhotra, V.M., Popovics, J.S., 2004 – Chapter 8, The Ultrasonic Pulse Velocity Method, CRC Handbook on nondestructive testing of concrete. Press LLC.
- Rio, J., Figueiras J., 2012 - Deteção de dano com ultrasons em elementos de betão estrutural. Encontro Nacional de Betão Estrutural (BE2012). Faculdade de Engenharia Universidade do Porto (FEUP), Portugal.
- Santos, M.J., 2004 - Ondas ultra-sonoras guiadas na caracterização e controlo não destrutivo de materiais. Dissertação para obtenção do Grau de Doutor em Engenharia Electrotécnica, na especialidade de Materiais e Campo Electromagnético. Faculdade de Ciências e Tecnologia. Universidade de Coimbra.
- Schickert, M., Krause, M., Müller, W., 2003 - Ultrasonic Imaging of Concrete Elements Using Reconstruction by Synthetic Aperture Focusing Technique. Journal of Materials in Civil Engineering © ASCE / MAY/JUNE 2003 pp. 235-246.